

Chaos synchronization in RCL-shunted Josephson junctions via a common chaos driving

Y.L. Feng^a and K. Shen

Department of Physics, Changchun University of Science and Technology, Changchun 130022, P.R. China

Received 18 July 2007 / Received in final form 23 October 2007

Published online 31 January 2008 – © EDP Sciences, Società Italiana di Fisica, Springer-Verlag 2008

Abstract. We study chaos synchronization in two resistive-capacitive-inductive-shunted (RCL-shunted) Josephson junctions (RCLSJJs) by using a common chaos driving. The numerical simulations confirm that the synchronization of two RCLSJJs can be achieved with a suitable driving intensity when the maximum condition Lyapunov exponent (MCLE) is negative.

PACS. 74.50.+r Tunneling phenomena; point contacts, weak links, Josephson effects – 05.45.Xt Synchronization; coupled oscillators – 05.45.Pq Numerical simulations of chaotic systems

1 Introduction

Since the seminal work by Huberman et al. [1], the study of chaos in Josephson junctions has attracted much attention due to their extensive applications [2,3]. Early, one model of Josephson junctions is resistive-capacitive-shunted junction (RCSJ) introduced by Stewart et al. [4], and its chaos behaviors have been reported in [5,6]. With the rapid development in fabrication technology and low temperature techniques, the Josephson junction with higher critical current could be expected in practical applications. To further study this kind of junctions, the RCLSJJ model was proposed by Whan et al. [7]. So the disadvantage of the RCSJ model has been modified. Then, there have been several reports on dynamics of RCLSJJ. Whan et al. [8] studied chaotic behavior and the effect of thermal noise in this system; Cawthorne et al. [9] investigated complex dynamics of RCLSJJ, also they [10] reported synchronized oscillations in RCLSJJ array. Recently, chaos control and chaotic synchronization in RCLSJJs have been the interesting subjects of research [11–13], since this kind of junctions are more used in secure communication and the Mixer systems [14,15]. Yang et al. [11] reported a computer-assisted proof of chaos in RCLSJJs; Dana et al. [12] reported taming of chaos and synchronization in RCLSJJs by external periodic forcing; Ucar et al. [13] reported chaos synchronization in RCLSJJs via active control. In addition, Zhou et al. [16] reported that common driving noise can induce complete synchronization and phase synchronization

in the Rossler system and Lorenz system. In this paper, we will study complete chaos synchronization in two RCLSJJs by using a common chaos driving. The numerical results show that two driven RCLSJJs can be synchronized with each other by properly adjusting driving intensity.

2 Chaos in RCL-shunted Josephson junction

The normalized dynamical equation of the RCLSJJ used here is the following [8]:

$$\begin{aligned}\frac{d\gamma}{d\tau} &= v \\ \frac{dv}{d\tau} &= \frac{1}{\beta_c}(i - gv - \sin(\gamma) - i_s) \\ \frac{di_s}{d\tau} &= \frac{1}{\beta_L}(v - i_s)\end{aligned}\quad (1)$$

where normalized time $\tau = \omega t$, with $\omega = 2eI_c R_s / \hbar$, γ is the phase difference of the superconducting order parameter across the junction.

- The normalized junction voltage: $v = V/I_c R_s$, and V is the junction voltage.
- The normalized external dc bias current: $i = I/I_c$.
- The normalized shunt current: $i_s = I_s/I_c$.

^a e-mail: fy10819@yahoo.com.cn

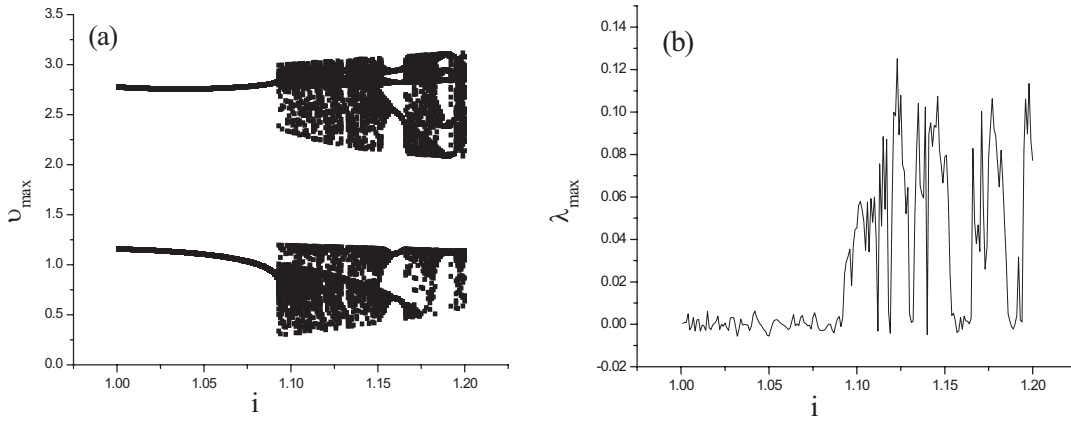


Fig. 1. (a) The bifurcation diagram of the RCLSJJ versus i ; (b) the maximum Lyapunov exponent $\lambda_{\max} - i$. Parameters: $\beta_c = 0.707$, $\beta_L = 2.68$, $g = 0.0478$.

Other dimensionless parameters are as follows:

$$\begin{aligned}\beta_c &= 2eI_c R_s^2 C / \hbar \\ \beta_L &= 2eI_c L / \hbar \\ g &= R_s / R_V.\end{aligned}$$

Here R_s and L are the shunt resistance and inductance, respectively. I , I_s , and I_c are the external dc bias current, the shunt current flowing through R_s , and the junction critical current, respectively. C and R_V are the junction capacitance and the junction resistance, respectively. \hbar is Planck constant.

To show chaotic behaviors in RCLSJJ system, equation (1) is solved with changing the bias current i for fixed $\beta_c = 0.707$, $\beta_L = 2.68$, and $g = 0.0478$. In this work, the differential equations are numerically solved by using the fourth-order Runge- Kutta method with a fixed step $\Delta\tau = 0.01$ and total steps $N_{step} = 10^5$, the Lyapunov exponents are computed by using the algorithms by Wolf [17], and the voltage bifurcation diagrams are plotted by recording the local maxima in the voltage time series [18]. The parametric values used in numerical calculations are obtained from [7] and [8] at temperature $T = 7.60$ K. The bifurcation diagram and the maximum Lyapunov exponent (MLE) versus the external bias current are presented in Figure 1, where one can find that for $1.090 < i < 1.156$ and $1.164 < i \leq 1.20$ the RCLSJJ system is in chaotic states which are occasionally interrupted by periodic windows; for other i values in the selected range, this system is in the periodic state. Thus, the state of this RCLSJJ can be changed by adjusting the external bias current.

3 The synchronization scheme and numerical simulations

The chaotic driving synchronization method was proposed in [19], where there are three systems, one is taken as the

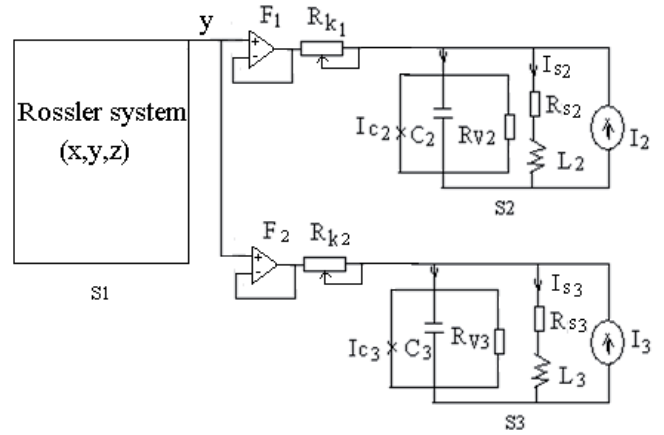


Fig. 2. Synchronization scheme.

drive system; the other two are taken as the driven systems. The output signal of the drive system is used to drive two driven systems. The synchronization of two systems is achieved when the MCEs of two driven systems are negative. Here we present the synchronization scheme of [19] for two RCLSJJs and give the numerical results for common autonomous chaos driving and common non-autonomous chaos driving.

3.1 Autonomous chaotic Rossler system as driving system

The schematic diagram is shown in Figure 2, where the drive system is different from the driven systems.

In Figure 2, the driving circuits are formed by R_{k1} , R_{k2} , F_1 , and F_2 [20]; S1 is chaotic Rossler circuit system and is taken as the drive system; S2 and S3 are two RCLSJJs and are regarded as driven systems, which have the same parameter values and different initial conditions. In order to make it convenient for numerical analysis, the

parameters of system S2 are used for normalizing to obtain dimensionless variables and parameters of systems S1, S2, and S3. So, the normalized time $\tau = \omega_2 t$, with $\omega_2 = 2eI_{c2}R_{s2}/\hbar$, all currents here are normalized to I_{c2} and all voltages to $I_{c2}R_{s2}$. The system S1 is not affected by the systems S2 and S3, and its equation is the following.

$$\begin{aligned}\frac{dx}{d\tau} &= -y - z \\ \frac{dy}{d\tau} &= x + ay \\ \frac{dz}{d\tau} &= b + xz - cz.\end{aligned}\quad (2)$$

Here x , y and z are normalized variables and are normalized voltages; a , b , and c are dimensionless parameters. For the systems S2 and S3, their dynamical behaviors are influenced by system S1, so their dynamics equations are changed, and their dimensionless equations are shown as follows.

$$\begin{aligned}\frac{d\gamma_n}{d\tau} &= v_n \\ \frac{dv_n}{d\tau} &= \frac{1}{\beta_{cn}}(i_n - g_n v_n - \sin(\gamma_n) - i_{sn} + k(y - v_n)) \\ \frac{di_{sn}}{d\tau} &= \frac{1}{\beta_{Ln}}(v_n - i_{sn}).\end{aligned}\quad (3)$$

Here $n = 2$ and $n = 3$ represent the systems S2 and S3, respectively.

- The normalized junction voltage: $v_n = V_n/I_{c2}R_{s2}$, and V_n is the junction voltage.
- The normalized external dc bias current: $i_n = I_n/I_{c2}$.
- The normalized shunt current: $i_{sn} = I_{sn}/I_{c2}$.

Other dimensionless parameters are the following:

$$\begin{aligned}\beta_{cn} &= 2eI_{cn}R_{sn}^2 C_n/\hbar \\ \beta_{Ln} &= 2eI_{cn}L_n/\hbar \\ g_n &= R_{sn}/R_{Vn}\end{aligned}$$

and the normalized driving intensity $k = \frac{R_{s2}}{R_{k1}} = \frac{R_{s3}}{R_{k2}}$. We may adjust appropriately R_{k1} and R_{k2} so as to obtain a driving signal with an appropriate intensity and achieve chaos synchronization in the driven systems.

To illustrate the synchronization process, we numerically analyze systems S1, S2, and S3 under condition of the system S1 being in chaotic state and systems S2 and S3 being in various dynamics states (periodic and chaotic) before being driven. Thus, the parameters of system S1 are chosen as follows: $a = b = 0.2$ and $c = 4.5$, with which system S1 lies in a chaotic state. According to Figure 1, in order to make original systems S2 and S3 stay in different states, we change their bias current from $i_2 = i_3 = 1.0$ to $i_2 = i_3 = 1.16$ and maintain $g_2 = g_3 = 0.0478$, $\beta_{c2} = \beta_{c3} = 0.707$, and $\beta_{L2} = \beta_{L3} = 2.68$. The initial values are: $x^0 = 1.0$, $y^0 = 1.1$, $z^0 = 1.0$, $\gamma_2^0 = 0.1$, $v_2^0 = 2.0$,

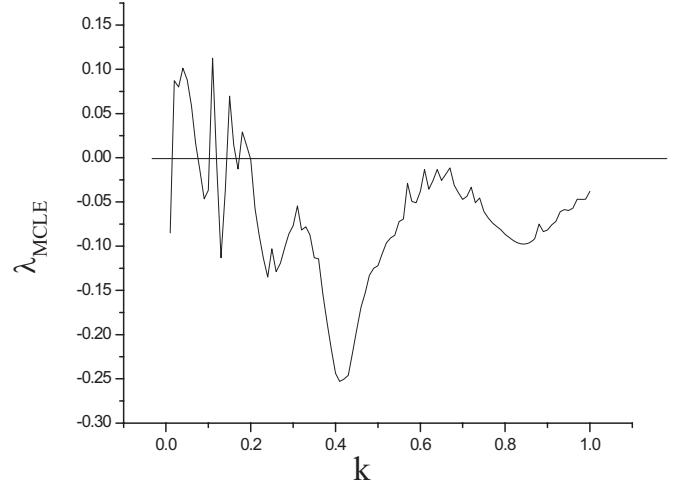


Fig. 3. The MLE of the driven systems S2 and S3 versus the driving intensity k with parameters $\beta_{c2} = \beta_{c3} = 0.707$, $g_2 = g_3 = 0.0478$, $i_2 = i_3 = 1.12$, $\beta_{L2} = \beta_{L3} = 2.68$, $a = b = 0.2$, and $c = 4.5$.

$i_{s2}^0 = 0.1$, $\gamma_3^0 = 0.2$, $v_3^0 = 2.2$, and $i_{s3}^0 = 0.2$. With the parametric values and initial values above, we solve equations (2) and (3). The numerical results show whether systems S2 and S3 were in periodic or chaotic states previously, when they are driven by system S1 with the driving intensity $k \geq 0.21$, they can enter into chaos synchronization states, i.e., $\gamma_2 = \gamma_3$, $v_2 = v_3$, and $i_{s2} = i_{s3}$. To show the synchronization phenomenon, now we take $i_2 = i_3 = 1.12$ with other parameter values being the same as those in Figure 1, and the MLE of driven systems S2 and S3 is shown in Figure 3.

In Figure 3, one can find that for $0.08 < k < 0.10$, $0.12 < k < 0.14$, and $0.21 \leq k \leq 1.0$, the MLE is negative, namely, two driven systems S2 and S3 can be synchronized with the value of k selected in these three ranges. The synchronization phenomenon with $k = 0.21$ can be clearly seen in Figure 4, where (a), (b), and (e), (f) are the attractors of systems S2 and S3 before and after they are driven, respectively. One can see that Figures 4e and 4f are influenced by the drive system and are different from Figures 4a and 4b. From Figure 4c we cannot see a regular relation between v_2 and v_3 , and the relationship is complex; from Figure 4d we can see that the difference of the $v_2 - v_3$ is not zero value for long time, so systems S2 and S3 are not synchronized before being driven. From Figures 4g and 4h, one can find $v_2 = v_3$, which always holds true after the transient process has died out, other corresponding variables are also the same, thus systems S2 and S3 are synchronized after being driven with $k = 0.21$.

In addition, we find that if the states of systems S2 and S3 vary with the bias current $i = i_2 = i_3$ before they are driven, the minimum value of the driving intensity k vary with them in order to make the synchronous chaos states exist in the driven systems S2 and S3. The relationship is plotted in Figure 5.

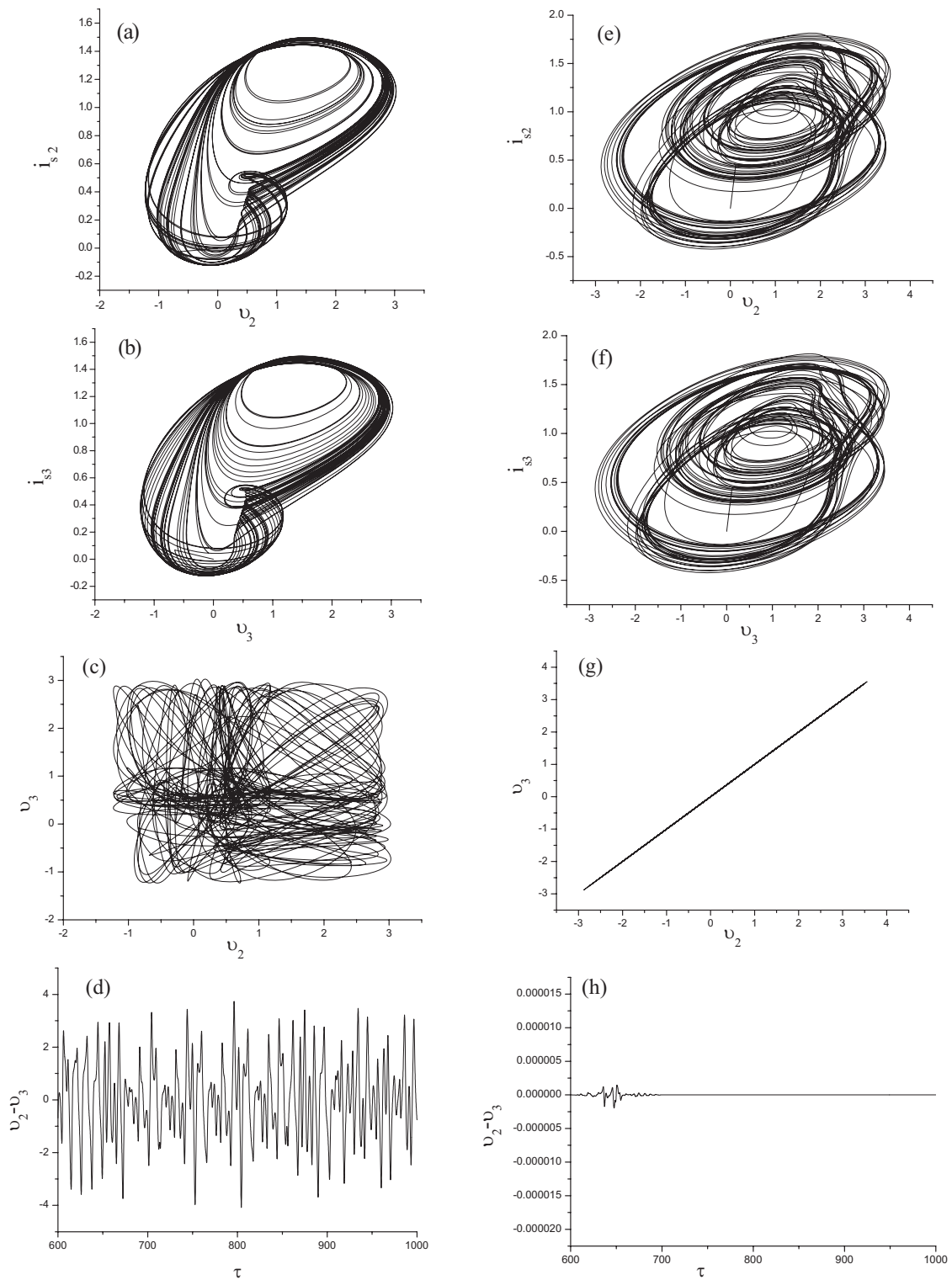


Fig. 4. Chaos synchronization in systems S2 and S3 before and after being driven with $k = 0.21$ and other parameters being the same as those in Figure 3. Here (a, b, e, f) the attractor on planes $v_2 - i_{s2}$ and $v_3 - i_{s3}$ before and after being driven; (c, g) the relation between v_2 and v_3 before and after being driven; (d, h) the difference of $v_2 - v_3$ versus time τ , before and after being driven, respectively.

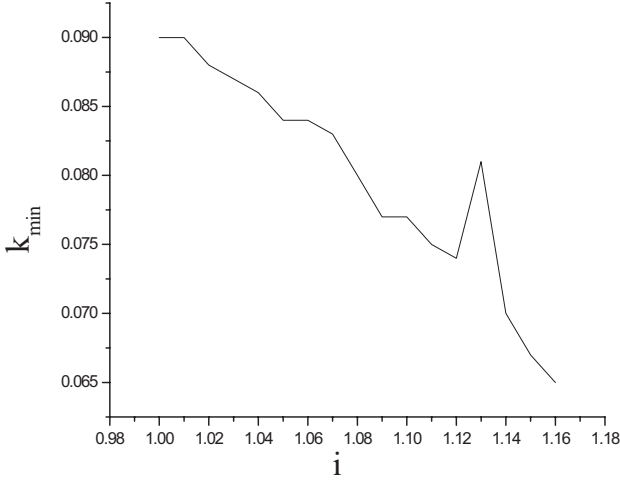


Fig. 5. The minimum driving intensity K_{\min} versus the bias current $i = i_2 = i_3$ with other parametric values being the same as those in Figure 3.

As the state of Rossler system can be changed by adjusting parameter c , we take different c values and obtain different chaos states in order to study chaos synchronization in systems S2 and S3. The numerical results show whether original systems S2 and S3 are chaotic or not, they can achieve chaos synchronization when the Rossler system is in chaotic state and the MCLEs of systems S2 and S3 are negative with proper driving intensity.

3.2 Non-autonomous chaotic RCSJ as driving system

The schematic diagram is shown in Figure 6, where systems S2 and S3 are two RCLSJJs which are the same as those in Figure 2; RCSJ is regarded as driving system.

Here we take the parameters of this RCSJ as follows [1]: $R_1 = 4 \Omega$, $C_1 = 5 \text{ pF}$, $I_{c1} = 100 \mu\text{A}$, and the plasma frequency $\omega_1 = (2eI_{c1}/\hbar C_1)^{1/2} = 10^{10} \text{ Hz}$. The parameters of system S2 are also used for normalizing, and normalized dynamical equation of RCSJ is the following [1]:

$$\begin{aligned} \frac{d\gamma_1}{d\tau} &= v_1 \\ \frac{dv_1}{d\tau} &= -g_{11}v_1 - g_{12}\sin(\gamma_1) + g_{12}\alpha \cos\left(\beta\frac{\omega_1}{\omega_2}\tau\right), \end{aligned} \quad (4)$$

where

$$\begin{aligned} g_{11} &= \frac{1}{C_1\omega_2 R_1} \\ g_{12} &= \frac{I_{c1}}{I_{c2}C_1\omega_2 R_{s2}}. \end{aligned}$$

The normalized junction voltage: $v_1 = V_1/I_{c2}R_{s2}$

$$\alpha = \frac{I_{a1}}{I_{c1}} \quad (5)$$

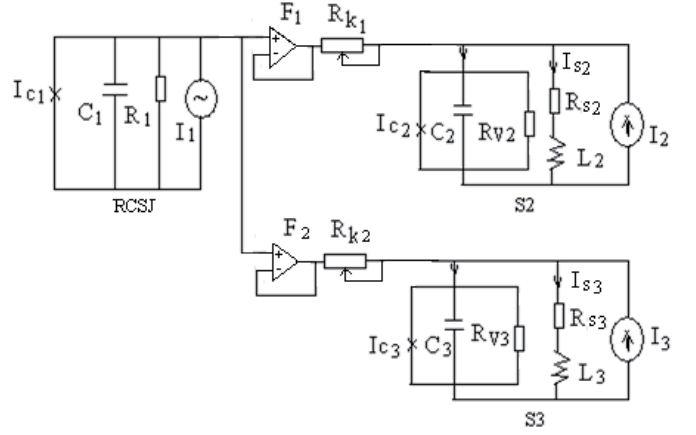


Fig. 6. Synchronization scheme.

$$\beta = \frac{\omega_{a1}}{\omega_1}, \quad (6)$$

where I_{a1} and ω_{a1} are respectively the amplitude and angle frequency of I_1 which is the external ac bias current, and $I_1 = I_{a1} \cos(\omega_{a1}t)$. From equation (4), it is found that α and β can be taken as the control parameters. According to equations (5) and (6), the values of α and β can vary with the change of the amplitude I_{a1} and frequency ω_{a1} , respectively. The RCSJ system can be in different dynamics states with different α or β values [1], so its dimensionless parameter values are chosen to be [1]: $g_{11} = 0.054$, $g_{12} = 0.0717$, $\alpha = 0.72$, $\beta = 0.55$, and $\frac{\omega_1}{\omega_2} = 0.2679$, for which this RCSJ is in chaotic state with the MLE being 0.02951. The parameters of systems S2 and S3 are chosen to be: $i_2 = i_3 = 1.0 \sim 1.16$, and other parameter values being the same as those in Figure 1. With this scheme and these parameter values above, we also carry out numerical simulations of chaos synchronization in two driven RCLSJJs. The results show whether systems S2 and S3 are chaotic or not before being driven, they can enter into the chaos synchronization state when they are driven by chaotic RCSJ with the driving intensity $k \geq 0.35$. The synchronization phenomenon with $k = 0.35$ and $i_2 = i_3 = 1.12$ can also be clearly seen in Figure 7.

Therefore, both autonomous chaos driving and non-autonomous chaos driving can induce chaos synchronization in two driven RCLSJJs. But the autonomous chaos driving is better, since (1) the driving intensity, which makes the synchronous chaos states exist in the driven RCLSJJs, is smaller than that one of the non-autonomous chaos driving; (2) autonomous chaos driving do not need additional ac current source.

Based on the results above, we extend chaos synchronization in two driven RCLSJJs to more driven RCLSJJs. As an example, the case of existing one driving system and three driven RCLSJJs is studied, and their parameters are the same as those above, but the initial conditions are different. The calculation results indicate that these three driven RCLSJJs can also be synchronized if their MCLEs are negative.

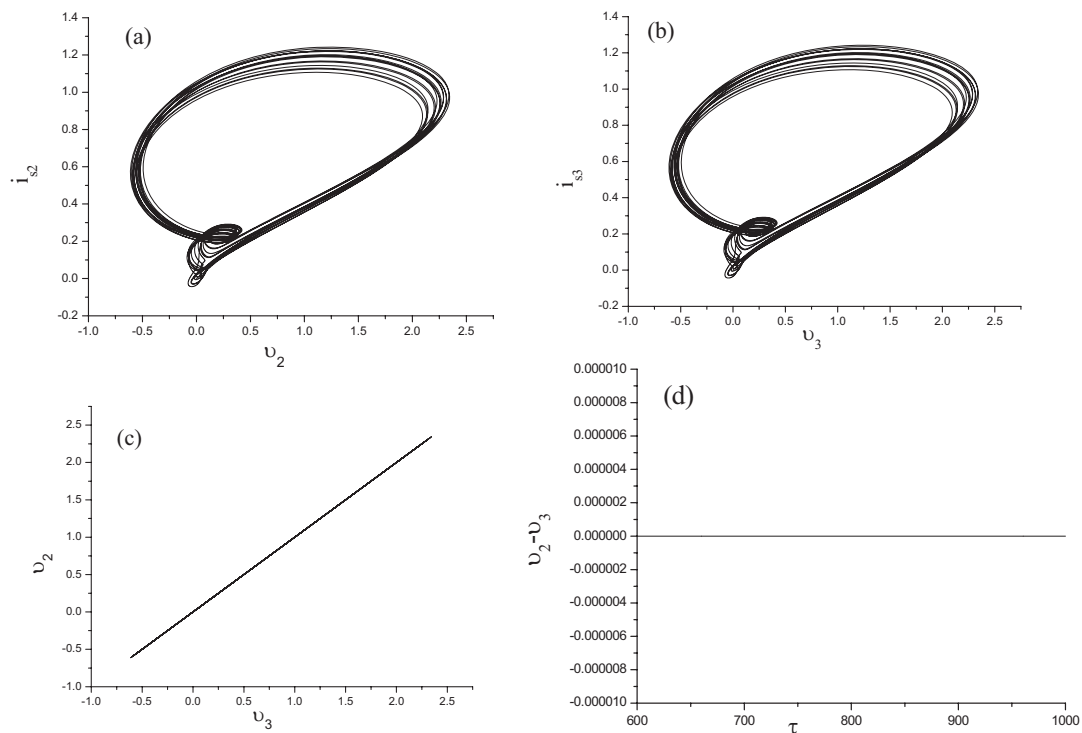


Fig. 7. Chaos Synchronization in driven systems S2 and S3 with $k = 0.35$, $g_{11} = 0.054$, $g_{12} = 0.0717$, $\alpha = 0.72$, $\beta = 0.55$, $\frac{\omega_1}{\omega_2} = 0.2679$, and other parameter values being the same as those in Figure 4. Here (a, b) the attractor on planes $v_2 - i_{s2}$ and $v_2 - i_{s3}$, respectively; (c) the relation between v_2 and v_3 ; (d) the difference of $v_2 - v_3$ versus times τ .

4 Conclusion

This paper has studied parameter conditions for chaos generation in RCLSJJ by changing external dc bias current and presented the scheme for chaos synchronization in two RCLSJJs by using a common chaos driving. Numerical results have demonstrated that both autonomous chaos driving and non-autonomous chaos driving can induce chaos synchronization in two or several driven RCLSJJs by choosing proper driving intensity. This is useful for achieving chaotic synchronization in RCLSJJs.

References

1. B.A. Huberman, J.P. Crutchfield, N.H. Packard, *Appl. Phys. Lett.* **37**, 750 (1980)
2. M.T. Levinsen, R.Y. Chiao, M.J. Feldman, B.A. Tucker, *Appl. Phys. Lett.* **31**, 776 (1977); B. Mao, Y.D. Dai, F.R. Wang, *Chin. Phys.* **14**, 301 (2005)
3. Z.Y. Shen, *High-Temperature Superconducting Microwave Circuits*, 1st edn. (National Defence Industry Publishing House, BeiJing, 2000), pp. 187–202
4. W.C. Stewart, *Appl. Phys. Lett.* **12**, 277 (1968)
5. M. Octavio, *Phys. Rev. B* **29**, 1231 (1984); H.D. Jensen, A. Larsen, J. Mygind, *Physica B* **165**, **166**, 1661 (1990); R.L. Kautz, J.C. Macfarlane, *Phys. Rev. A* **33**, 498 (1986)
6. J.A. Blackburn, G.L. Baker, H.J.T. Smith, *Phys. Rev. B* **62**, 5931 (2000)
7. C.B. Whan, C.J. Lobb, M.G. Forrester, *J. Appl. Phys.* **77**, 382 (1995)
8. C.B. Whan, C.J. Lobb, *Phys. Rev. E* **53**, 405 (1996)
9. A.B. Cawthorne, C.B. Whan, C.J. Lobb, *J. Appl. Phys.* **84**, 1126 (1998)
10. A.B. Cawthorne, P. Barbara, S.V. Shitov, C.J. Lobb, K. Wiesenfeld, A. Zangwill, *Phys. Rev. B* **60**, 7575 (1999)
11. X.S. Yang, Q. Li, *Chaos Solitons Fractals* **27**, 25(2006)
12. S.K. Dana, P.K. Roy, G.C. Sethia, A. Sen, D.C. Sengupta, *IEE Pro. Circuits Devices Syst.* **153**, 453(2006)
13. A. Ucar, K.E. Lonngren, E.W. Bai, *Chaos Solitons Fractals* **31**, 105(2007)
14. S.P. Benz, C. Burroughs, *Appl. Phys. Lett.* **58**, 2162 (1991)
15. I. Siddiqi, R. Vijay, F. Pierre, C.M. Wilson, L. Frunzio, M. Metcalfe, C. Rigetti, R.J. Schoelkopf, M.H. Devoret, D. Vion, D. Esteve, *Phys. Rev. Lett.* **94**, 027005 (2005)
16. C. Zhou, J. Kurths, *Phys. Rev. Lett.* **88**, 230602-1 (2002)
17. A. Wolf, J.B. Swift, H.L. Swinney, J.A. Vastano, *Physica* **16D**, 285 (1985)
18. J.C. Sprott, *Phys. Lett. A* **228**, 271 (1997)
19. R. Wang, K. Shen, *Phys. Rev. E* **65**, 016207 (2001)
20. Z. Wang, *Journal of Superconductivity* **17**, 233 (2004)